Biochimica et Biophysica Acta 1788 (2009) 1159–1167

Contents lists available at ScienceDirect

Biochimica et Biophysica Acta

journal homepage: www.elsevier.com/locate/bbamem

Solid-state NMR and molecular dynamics characterization of cannabinoid receptor-1 (CB1) helix 7 conformational plasticity in model membranes

Elvis K. Tiburu [a], Anna L. Bowman [a], Jochem O. Struppe [b], David R. Janero [a], Hava K. Avraham [c], Alexandros Makriyannis [a,*]

[a] Center for Drug Discovery, Northeastern University, Boston, MA 02115, USA
[b] NMR Division, Bruker Biospin Corporation, Billerica, MA 01821, USA
[c] Beth Israel Deaconess Medical Center, Boston, MA 02115, USA

ARTICLE INFO

Article history:
Received 31 October 2008
Received in revised form 30 January 2009
Accepted 2 February 2009
Available online 12 February 2009

Keywords:
GPCR structure
Human cannabinoid receptor
NMR
Molecular dynamics simulation
Membrane
Protein conformation
Hydrophobic mismatch

ABSTRACT

Little direct information is available regarding the influence of membrane environment on transmembrane (TM) G-protein-coupled receptor (GPCR) conformation and dynamics. The human CB1 cannabinoid receptor (hCB1) is a prominent GPCR pharmacotherapeutic target in which helix 7 appears critical to ligand recognition. We have chemically synthesized a hCB1 peptide corresponding to a segment of TM helix 7 and the entire contiguous helix 8 domain (fourth cytoplasmic loop) and reconstituted it in defined phospholipid-bilayer model membranes. Using an NMR-based strategy combined with molecular dynamics simulations, we provide the first direct experimental description of the orientation of hCB1 helix 7 in phospholipid membranes of varying thickness and the mechanism by which helix-7 conformation adjusts to avoid hydrophobic mismatch. Solid-state ^{15}N NMR data show that hCB1 helices 7 and 8 reconstituted into phospholipid bilayers are oriented in a TM and in-plane (i.e., parallel to the phospholipid membrane surface) fashion, respectively. TM helix orientation is influenced by the thickness of the hydrophobic membrane bilayer as well as the interaction of helix 8 with phospholipid polar headgroups. Molecular dynamics simulations show that a decrease in phospholipid chain-length induces a kink at P394 in TM helix 7 to avoid hydrophobic mismatch. Thus, the NP(X)nY motif found in hCB1 and highly conserved throughout the GPCR superfamily is important for flexing helix 7 to accommodate bilayer thickness. Dynamic modulation of hCB1-receptor TM helix conformation by its membrane environment may have general relevance to GPCR structure and function.

© 2009 Elsevier B.V. All rights reserved.

1. Introduction

Incorporation of a protein transmembrane (TM) domain into a membrane lipid bilayer is driven by the hydrophobic effect associated with free-energy minimization of the system and the interplay between the hydrophobic length of the membrane-spanning protein segment and the thickness of the membrane phospholipid bilayer [1–3]. Discrepancy between the length of the hydrophobic domain of a membrane-spanning protein and bilayer thickness ("hydrophobic mismatch") has adverse consequences for cellular processes such as protein sorting along the secretory pathway and membrane stability [4]. Hydrophobic mismatch may also influence the orientation of protein TM helices as a function of their hydrophobic length, an effect observed at the molecular level in model systems involving synthetic hydrophobic peptides and hydrated membrane vesicles composed of phospholipids with differing chain lengths [5–7].

Hydrophobic mismatch can be compensated for in various ways [6,8,9]. The membrane bilayer region surrounding the imbedded protein segment may adjust its thickness in accord with the length of the hydrophobic TM protein region. Should the length of the protein's TM region exceed the thickness of its surrounding lipid bilayer, either protein tilting or a kink at a proline residue would reduce its effective length across the bilayer. Proline residues are well-known α-helical destabilizers in globular proteins, and many biologically important peptide sequences contain proline [10]. For example, the NP(X)nY motif conserved throughout the G-protein-coupled receptor (GPCR) superfamily is considered to play a significant role in signal transduction at the level of select GPCR TM helices [10,11].

The endogenous cannabinoid (CB) (endocannabinoid) signaling system is implicated in a variety of (patho)physiological processes,

Abbreviations: hCB1, human CB1 cannabinoid receptor; GPCR, G-protein-coupled receptor; HEPES, N-[2-hydroxyethylpiperazine-N′-2-ethane]sulfonic acid; TFE, trifluoroethanol; MD, molecular dynamics; SUV, small unilamellar vesicle; SPC, simple point charge; POPC, 1-palmitoyl-2-oleoyl-*sn*-glycero-3-phospocholine; DMPC, 1,2-dimyristoyl-*sn*-glycero-3-phosphocholine; TM, transmembrane; DPC, dodecylphosphocholine; Fmoc, 9*H*-fluoren-9-ylmethoxycarbonyl; CD, circular dichroism; RMSD, root-mean-square deviation

* Corresponding author. Tel.: +1 617 373 4200; fax: +1 617 373 7493.
E-mail address: a.makriyannis@neu.edu (A. Makriyannis).

0005-2736/$ – see front matter © 2009 Elsevier B.V. All rights reserved.
doi:10.1016/j.bbamem.2009.02.002

primarily by virtue of natural, arachidonic acid-derived lipids (endocannabinoids) that function as agonists for two membrane-bound, metabotropic CB GPCRs of the 1A, rhodopsin-like family. The general architecture of these CB receptors is defined by an extracellularly oriented N-terminus, an intracellular carboxyl terminus, and a counterclockwise arrangement of seven hydrophobic TM α-helices which span the cell membrane and are connected by three extracellular and three cytoplasmic loops [12,13]. The CB1 receptor subtype is the most abundant brain GPCR and centrally controls motor, cognitive, emotional, and sensory functions to influence pain perception, hormonal activity, thermoregulation, and cardiovascular, gastrointestinal, and respiratory physiology. Activation of central CB1 receptors also mediates most cannabinoid psychotropic and behavioral effects that reflect the psychoactivity of the marijuana phytocannabinoid, Δ^9-tetrahydrocannabinol. CB1 receptors at various peripheral sites (e.g., liver, adipocytes, endocrine pancreas) help regulate energy metabolism and other fundamental physiological processes [13,14]. Hyperactive CB1-receptor transmission has been implicated in many common diseases having a reward-supported component, such as overweight/obesity and substance abuse disorders [15]. Indeed, the first major drug to emerge from rational discovery efforts aimed at endocannabinoid-system modulation reached the market as a CB1-receptor antagonist for weight-control [16]. The CB1 receptor, accordingly, has gained intense current interest in medicinal chemistry as a therapeutic target for designer ligands and as the focus of research aimed at defining its ligand-binding architecture for therapeutic gain [15,17].

Four potential pharmacological modes of CB1 receptor–ligand interaction have been recognized: agonism, inverse agonism, antagonism, and allosterism [13,18]. Ligand binding motifs and pharmacological responses for the CB1 receptor and other GPCRs have been attributed to specific GPCR TM helix conformations and orientations within the cell membrane bilayer [19,20]. Conformational exchange in the micro-millisecond regime is important to the binding and pharmacodynamics of GPCR ligands, and helices 7 and 8 are considered critical to the stability of the GPCR-G-protein interaction at the cytoplasmic C-terminus [21]. Thus, information on GPCR TM helix structure and orientation appears essential to understanding the (patho)physiological roles of endogenous cannabinoids and elucidating the pharmacophore requirements for synthetic CB1-receptor ligands as potential drugs. Largely because of inherent difficulties in isolating structurally preserved GPCRs from their membrane environments for analysis by X-ray crystallography and nuclear magnetic resonance (NMR) spectroscopy, direct, experimentally-derived data on GPCR structure and ligand recognition are limited. Notwithstanding descriptions of the crystal structures of bovine rhodopsin [22], an engineered, human β2-adrenergic receptor [23], the ligand-free opsin receptor [24], and the β_1-adrenergic receptor–cyanopindolol complex [25], the structural details and conformational plasticity of CB receptors remain incompletely understood. The three-dimensional rhodopsin structure has been employed to derive CB-receptor homology models, which must remain speculative due to the attendant extrapolations involved [26–28]. Although some features of the CB1 receptor are reminiscent of rhodopsin and other GPCRs [22,27,29], the orientations of CB1-receptor helices need not be identical to those of other GPCRs whose three-dimensional structures have been solved. Computational and mutation studies have predicted the importance of helices 7 and 8 to CB1-receptor structure and function [29–31] and, in particular, the influence of helix-7 conformation to CB1-receptor ligand recognition [29,32,33]. These considerations mandate direct experimental characterization of the orientation of CB1-receptor TM helices within the membrane lipid environment and the factors influencing helix orientation and CB1 receptor-membrane cooperativity.

Chemically synthesized peptides corresponding to TM segments of naturally-occurring membrane proteins in aligned phospholipid-bilayer model membranes have proven to be useful experimental systems for gaining insight into the secondary structure of such proteins [34,35]. We have previously provided evidence that CB1-receptor helix 8 assumes an α-helical character in an amphipathic environment [29]. In this study, we have synthesized a human CB1 (hCB1) receptor fragment, hCB1(T377-E416), consisting of a segment of TM helix 7 and the entire helix 8 and reconstituted this peptide into phospholipid bilayers of known compositions. By utilizing circular dichroism spectropolarimetry (CD), solid-state NMR spectroscopy, and molecular dynamics (MD) simulations, we detail the orientation of hCB1 helix 7 in these bilayer membrane mimetics and identify some of the peptide's conformational determinants. Mechanically oriented, selectively ^{15}N-labeled hCB1(T377-E416) peptides allowed us to demonstrate unambiguously the presence of two α-helical peptide components at almost orthogonal orientation within 1,2-dimyristoyl-*sn*-glycero-3-phosphocholine (DMPC; 1,2–14:0) and 1-palmitoyl-2-oleoyl-*sn*-glycero-3-phospocholine (POPC; 1–16:0, 2–18:1) phospholipid bilayer environments. To determine the precise orientation of TM helix 7, the chemical shifts of six singly ^{15}N-labeled, mechanically oriented hCB1(T377-E416) peptides were studied in DMPC and POPC phospholipid bilayers. The ^{15}N chemical shifts obtained from the six singly labeled spectra were used to define the helical tilt of the hCB1 (T377-E416) peptide. Finally, MD simulations of hCB1(T377-E416) in DMPC and POPC bilayers were performed. To the authors' best knowledge, this is the first application of solid-state NMR spectroscopy to characterize directly the structural dynamics of CB-receptor helices within (model) membranes.

2. Materials and methods

2.1. Materials

POPC and DMPC in chloroform were purchased from Avanti Polar Lipids (Alabaster, AL) and stored at −20 °C. 2,2,2-Trifluoroethanol (TFE), N-[2-hydroxyethylpiperazine-N′-2-ethane]sulfonic acid (HEPES), and EDTA were obtained from Sigma-Aldrich (Milwaukee, WI). Deuterium-depleted water was purchased from Sigma-Aldrich (St. Louis, MO). Dodecylphosphocholine (DPC) was purchased from Cambridge Isotopic Laboratories (Andover, MA). All other chemicals were purchased from Sigma-Aldrich at highest available grade.

2.2. Peptide synthesis and purification

The numbering system of Bramblett et al. is employed [28]. Peptide corresponding to hCB1(T377-E416) (TVFAFCSMLCLLNSTVNPIIYALRSKDLRHAFRSMFPSCE) was synthesized using a 433A Peptide Synthesizer (Applied Biosystems, Foster City, CA) equipped for 9*H*-fluoren-9-ylmethoxycarbonyl (Fmoc) chemistry at the Molecular Biology Core Facility, Dana-Farber Cancer Institute (Boston, MA). All amino acids were single coupled, with a total of 9.5 min for the coupling and monitoring module. The peptide was purified on a Dynamax SD-200 LC system (Varian Instruments, Walnut Creek, CA) equipped with an Applied Biosystems 1000S diode array detector and Dynamax Method Manager (version 1.4.6) software and analyzed by MALDI-TOF mass spectrometry using an α-cyano-4-hydroxycinnamic acid calibration matrix. As estimated from the LC and MALDI-TOF data, peptide purity was 95% (data not shown).

2.3. Circular dichroism spectropolarimetry (CD)

The conformation of the hCB1(T377-E416) peptide was determined by CD using a nitrogen-flushed J-810 spectropolarimeter controlled by Spectra Manager software (version 1.15.00) (Jasco Instruments, Easton, MD) [36]. Although not capable of providing the residue-specific information available from NMR and X-ray crystallography, CD measurements can be made on small amounts

of material in physiological buffers, and structural alterations resulting from changes in environmental conditions (e.g., pH, temperature) can be monitored [37]. The peptide concentration was 60 μM. A 1-cm quartz cuvette (1-mm pathlength) was used, and the HT voltage was set at 120 mV. The spectra were recorded from 280 to 185 nm at 35 °C with a scan rate of 1 nm/min and an average of 10 scans per sample. The percentage α-helical content was calculated using the following equation:

$$\%\text{helix} = 100\times(\theta_{obs}-\theta_C)/(\theta_H-\theta_C),$$

where

$$\theta_H = -40,000\times(1-x/n) + 100T$$

and

$$\theta_C = 640-45T.$$

The quantities θ_H and θ_C represent the molar ellipticity values (deg-cm^2/dmol) for 100% α-helical and 100% random coil, respectively. The quantity θ_{obs} is molar ellipticity measured at 222 nm; n is the number of amino acids, T is the temperature in Kelvin, and the constant $x = 2.5$ [38].

2.4. NMR sample preparation

POPC and DMPC bilayers were prepared with a 2 mol% peptide-to-lipid ratio, i.e., with a peptide:lipid molar ratio of 1:50 [39–42]. The ^{15}N NMR powder sample was then transferred and packed into a 4-mm ZrO_2 rotor. A hydrated sample was prepared by placing the rotor containing the dry sample in a humidified (~93%) chamber of saturated ammonium monophosphate. The sample was then incubated for 6–12 h at 45 °C. A mechanically aligned sample was prepared by dissolving the hCB1(T377-E416) peptide in a minimal amount of TFE and mixing the resulting solution with either POPC or DMPC dissolved in chloroform (20 mg/ml) in a pear-shaped flask at a 1:50 peptide-to-lipid molar ratio. Nitrogen gas was passed through the resulting mixture until the volume of chloroform was reduced by two-thirds. The resulting sample was spread on 25 glass plates (8.5 mm × 14 mm), which were dried in a desiccator overnight [35]. Deuterium-depleted water was added to the lipid–peptide mixture, and the glass plates were stacked on top of one another. The stacked glass plates were then placed into a humidified ammonium monophosphate chamber (relative humidity ~93%; 42 °C) until the sample became transparent, indicating complete peptide incorporation into the phospholipid membrane. ^{31}P NMR of mechanically aligned DMPC and POPC samples in the presence of the peptide indicated that the phospholipids were well aligned with the bilayer normal, parallel to the external magnetic field (data not shown).

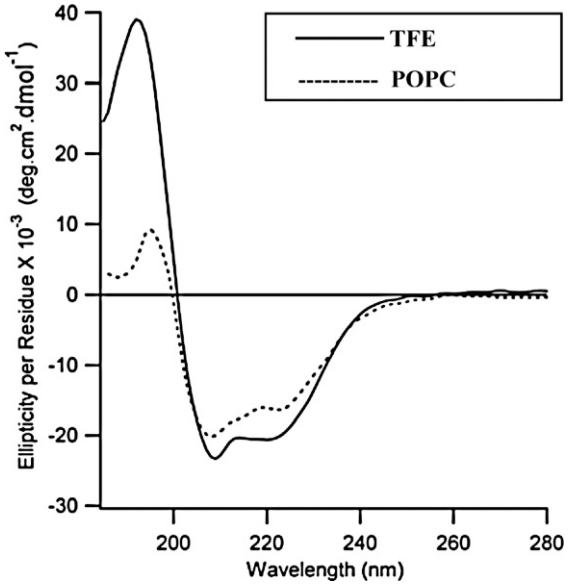

Fig. 1. CD of hCB1(T377-E416) peptide in trifluoroethanol (TFE) and in 1-palmitoyl-2-oleoyl-*sn*-glycero-3-phospocholine (POPC) small unilamellar vesicles (SUVs). CD spectra of the hCB1(T377-E416) peptide measured in 100% TFE (solid line) and in POPC SUVs with peptide-to-lipid ratio of 1:50 (dotted line) are shown. Spectra are the average of 10 scans.

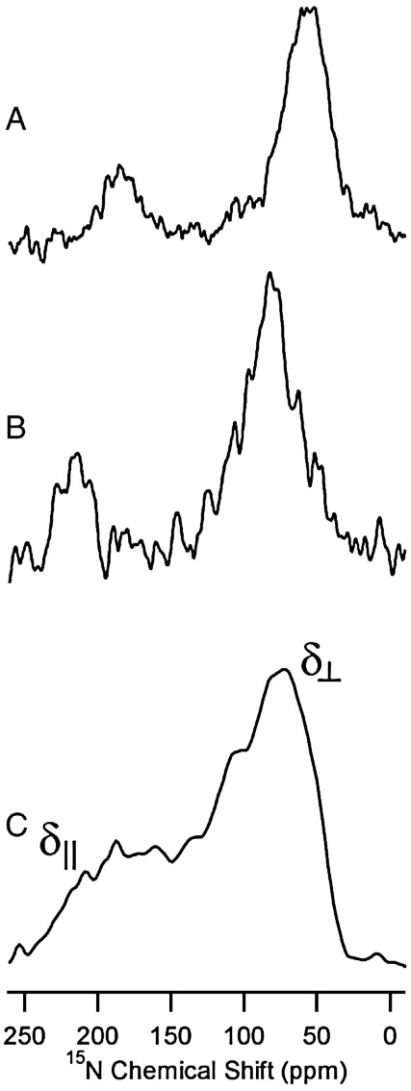

Fig. 2. One-dimensional chemical-shift ^{15}N NMR spectra of hCB1(T377-E416) peptide in phospholipid bilayers. (A) The spectrum corresponding to selectively labeled ^{15}N-[A380, A398, K402, L404, A407, M411]hCB1(T377-E416) in oriented DMPC bilayers. (Residues were selected to correspond to the cytosolic segments.) (B) The spectrum corresponding to selectively labeled ^{15}N-[A380, A398, K402, L404, A407, M411]hCB1(T377-E416) in oriented POPC bilayers. (C) The spectrum corresponding to selectively labeled ^{15}N-[A380, A398, K402, L404, A407, M411]hCB1(T377-E416) in unoriented POPC bilayers.

2.5. NMR spectroscopy

Solid-state ^{15}N NMR unoriented spectra were collected utilizing a standard cross polarization pulse sequence with ^{1}H decoupling between 60 and 80 kHz and a ^{1}H–^{15}N field strength of 50 kHz. For mechanically aligned samples, a double resonance flat coil probe was used operating at the required temperature in a 700 MHz spectrometer. For the DMPC bilayer sample, the following pulse

sequence parameters were used: 4.5 μs ^{1}H 90° pulse, 1.0 ms contact time, 600 ppm sweep width, and a 4 s recycle delay with ^{1}H decoupling. The 24 k scans were averaged and 300 Hz line broadening was used to process the data. For the POPC sample, the following pulse sequence parameters were used: 4.7 μs ^{1}H 90° pulse, 1.5 ms contact time, 500 ppm sweep width, and a 4 s recycle delay with ^{1}H decoupling [43]. The helical tilt angles for ^{15}N NMR spectra were calculated using equations previously derived in the literature [44–47].

2.6. MD simulation setup

Two explicit membrane–water environments were used, POPC and DMPC. A fully-solvated, pre-equilibrated bilayer of 128 DMPC lipids and 3655 water molecules (taken from http://moose.bio.ucalgary.ca/files/dmpc_npat.pdb) was found to be sufficiently large for the simulation in DMPC. Using a similarly sized POPC box, we noticed that the lateral diffusion of the hCB1(T377-E416) peptide in the POPC bilayer during unrestrained dynamics caused the peptide to move outside of the box. As we were concerned about any periodic artifacts that may occur from the limited size of the box, a larger POPC bilayer was produced by replicating and then truncating a fully pre-equilibrated $8\times8\times2$ POPC patch [48] in PyMOL (DeLano Scientific LLC, Palo Alto, CA). This yielded a fully-solvated POPC bilayer composed of 256 POPC lipid and 7016 water molecules. The POPC system was fully minimized with steepest descent, then 2 ns of MD were performed with the phosphorus atom of each lipid positionally constrained with a force constant of 1000 kJ mol^{-1} nm^{-2}. A further 2 ns of unrestrained MD were performed to produce a fully-solvated, fully-equilibrated POPC bilayer prior to peptide insertion (see MD details below). The potential energy reached a stable plateau after 700 ps, and the area of the *xy* plane per POPC lipid fluctuated around 61.3 Å^2, which is comparable to the experimental value of 63 Å^2 [49]. A refined hCB1(T377-E416) model was constructed using the rhodopsin crystal structure (PDB ID: 1L9H) [42] as a template in the "Prime" software package, 1.6 edition (Schrödinger, Inc., New York, NY).

2.7. MD simulation procedure

hCB1(T377-E416) was embedded into each of the pre-equilibrated POPC and DMPC lipid bilayers. Helix 7 was placed spanning the membrane, and helix 8 was oriented along the plane of the membrane, as suggested by homology modeling [27,28,32]. Any lipids or water molecules clashing with the peptide were removed. Each system was made electrically neutral by replacing two water molecules at the most positive electrostatic potential with two chloride ions and was minimized with steepest descents to relax unfavorable contacts between molecules. To achieve stability of the lipid environment during production dynamics, equilibration MD was performed for 2 ns, with all heavy atoms in the peptide positionally restrained with a force constant of 1000 kJ mol^{-1} nm^{-2}. Unconstrained production MD was performed for 10 ns on each system.

All MD simulations were performed in the NPT (isothermal–isobaric) ensemble with periodic boundary conditions. A temperature of 298 K was maintained by a Berenden thermostat [50] with time constant 0.1 ps. Semi-isotropic pressure coupling was used, with the reference pressure set at 1.0 bar and time constant 5 ps. Coulomb and short-range neighbor list cut-offs were both set to 0.9 nm, and Lennard-Jones cut-offs were set to 1.2 nm. The electrostatic interactions were computed with the Particle-Mesh Ewald method [51,52]

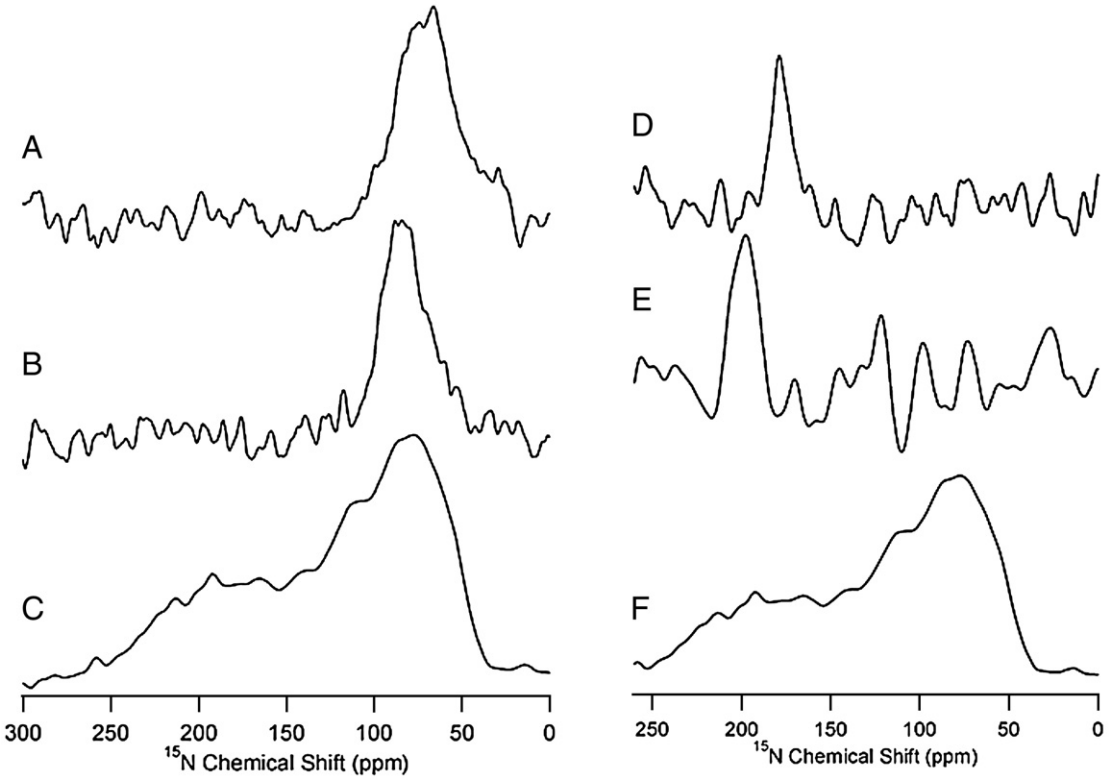

Fig. 3. One-dimensional chemical-shift ^{15}N NMR spectra of hCB1(T377-E416) peptide in phospholipid bilayers. (A) The spectrum corresponding to selectively labeled ^{15}N-[K402, L404, A407, M411]hCB1(T377-E416) in oriented DMPC bilayers. (B) The spectrum corresponding to selectively labeled ^{15}N-[K402, L404, A407, M411]hCB1(T377-E416) in oriented POPC bilayers. (C) The spectrum corresponding to selectively labeled ^{15}N-[K402, L404, A407, M411]hCB1(T377-E416) in unoriented POPC bilayers. The spectrum corresponding to selectively labeled ^{15}N-[A380]hCB1(T377-E416) in oriented DMPC bilayers (D) and in oriented POPC bilayers (E). (F) Chemical shift tensor of unoriented ^{15}N-[A380]hCB1(T377-E416) in POPC.

with an interpolation order of 4 and a maximum grid spacing of 0.12 nm. A time-step of 2 fs was used, and pair lists were updated every 10 steps. The LINCS algorithm [53] was employed to preserve bond lengths. The simple point charge water model [54] was used in all simulations. The lipid force field parameters were taken from Berger et al. and Chiu et al. [55,56], and the peptide used the GROMOS96 force field [57]. All simulations were carried out with the GROMACS program, version 3.2.1 [58,59].

2.8. Simulation analysis

During the production phase of MD, snapshots were taken every 2 ps, resulting in 5000 snapshots for each 10 ns trajectory. The top of helix 7 was defined as the center of mass of the five C_α atoms of residues V378, F379, A380, F381, and C382 of the hCB1(T377-E416) peptide. The other end was described by the center of mass of the five C_α atoms of I395, I396, Y397, A398 and L399. Similarly, the inception

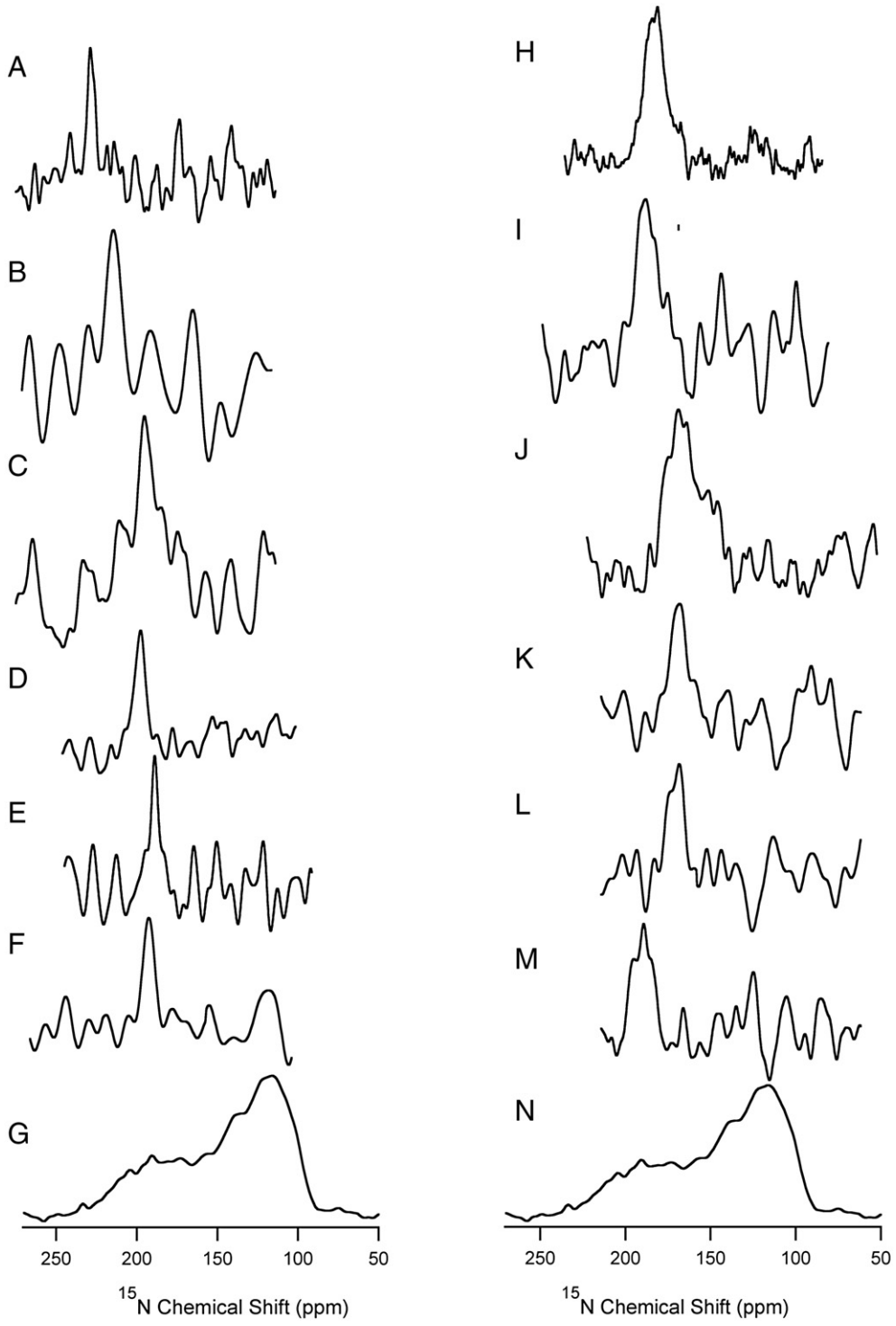

Fig. 4. One-dimensional solid-state ^{15}N NMR spectra of site-specifically ^{15}N-labeled hCB_1(T377-E416) in oriented DMPC and POPC phospholipid bilayers. The ^{15}N-labeled spectra displayed were collected at 35 °C for both DMPC and POPC bilayers. (A) V378, (B) A380, (C) L388, (D) V392, (E) A398, (F) L399, and (G) chemical shift tensor of unoriented, selectively ^{15}N-labeled hCB1(T377-E416) in POPC. The corresponding spectra of each of the six labeled peptides in DMPC phospholipid bilayers are displayed. (H) V378, (I) A380, (J) L388, (K) V392, (L) A398, (M) 399, and (N) chemical shift tensor of unoriented, selectively ^{15}N-labeled hCB1(T377-E416) in DMPC. The spectra were referenced to external $^{15}NH_4(SO_4)_2$ at 27 ppm.

of helix 8 was defined using the center of mass of the five C_α atoms of residues D403, L404, R405, H406 and A407, and the other end was described by the center of mass of the five C_α atoms of F408, R409, S410, M411 and F412. With these definitions, the tilt of helix 7 relative to the membrane axis and the angle between helices 7 and 8 were calculated using the g_bundle analysis tool in GROMACS [58,59].

3. Results and discussion

3.1. Secondary structure of hCB1(T377-E416) in phospholipid bilayer model membranes

CD is a key method for measuring peptide helix formation, since CD spectra reflect the quantity of peptide secondary structure (α-helices, β-sheets, β-turns) [37]. The CD spectra of the peptide 40-mer corresponding to hCB1(T377-E416) in TFE and POPC evidenced two bands at 192 nm and 220 nm, characteristic of an α-helical structure (Fig. 1). The α-helical content of hCB1(T377-E416) was calculated to be 67% in TFE and 41% in POPC. The lower α-helical content in the latter instance may be due to a scattering effect of the phospholipids. This result is in accord with a previous observation [29] that the CB1-receptor helix 8 assumes an α-helical character in an amphipathic environment.

3.2. ^{15}N NMR analysis of hCB1(T377-E416) orientation in DMPC and POPC bilayers

Proton-decoupled solid-state ^{15}N NMR spectroscopy of oriented membrane peptides is useful for investigating polypeptide backbone secondary structure and topology [39]. The NMR spectrum in Fig. 2A was obtained at 35 °C from an oriented sample of hCB1(T377-E416) peptide with six ^{15}N-labeled residues (A380, A398, K402, L404, A407, M411) in DMPC bilayers mechanically aligned on glass plates. There are two relatively broad resonances in the spectrum due to the six ^{15}N-labeled residues which appear at 185 and 60 ppm, respectively. Fig. 2B was obtained from six ^{15}N-labeled hCB1(T377-E416) peptide residues in aligned POPC bilayers and also exhibits two broad resonances, with chemical shifts at 215 and 83 ppm. The resonance peak-intensity ratio for the spectra in Fig. 2A and B is ~1:2. Their chemical shift values suggest that two out of the six ^{15}N-labeled amino acid residues are oriented with the long molecular axis parallel to the bilayer normal and the external magnetic field, whereas the other four residues are oriented perpendicular to the bilayer normal. Fig. 2C represents the same six ^{15}N-labeled hCB1(T377-E416) peptide in unoriented POPC phospholipid bilayers and is used for direct comparison of the frequencies that provided the orientational constraints in Fig. 2A and B. Here, the unoriented spectrum spans from 225 to 50 ppm, indicative of a peptide backbone that is quite rigid within the membrane in the NMR time scale. The aggregate NMR data in Fig. 2 suggest that the hCB1(T377-E416) peptide in DMPC and POPC bilayers encompasses membrane-spanning hydrophobic and membrane-flanking hydrophilic regions.

In order to identify which of the above six labeled residues are either embedded within or disposed externally to the bilayer, we synthesized hCB1(T377-E416) with one ^{15}N label at A380 and another peptide with four ^{15}N labels at K402, L404, A407 and M411 and separately incorporated the labeled peptides into oriented DMPC or POPC subtypes. As shown in Fig. 3A, ^{15}N-[K402, L404, A407, M411] hCB1(T377-E416) evidences an in-plane helix with its N–H resonance at 60 ppm and near the upfield end (δ_{11}) of the powder pattern spectrum (Fig. 3C) in DMPC. Fig. 3B shows the orientation of ^{15}N-[K402, L404, A407, M411]hCB1(T377-E416) in POPC, which displays an in-plane N–H bond resonance peak at 83 ppm. The average chemical shift of ~70 ppm from the membrane preparations is reflective of a peptide residing practically on the membrane surface. ^{15}N-[A380] hCB1(T377-E416) was separately incorporated into DMPC and POPC bilayers to determine the orientation of the TM peptide in these two lipid environments. In DMPC, ^{15}N-[A380]hCB1(T377-E416) displayed a chemical shift at 185 ppm (Fig. 3D) and a resonance at 215 ppm in POPC (Fig. 3E) near the downfield end (δ_{33}) of the powder pattern spectrum (Fig. 3F). The results are consistent with the spectra in Fig. 2 and also with the MD simulation data (below), indicating that the helix 7 microdomain (T311-L399) (which includes ^{15}N-[A380]) is in a transmembrane orientation, whereas helix 8 (D403-F412) (which includes ^{15}N-[K402, L404, A407, and M411]) is oriented along the plane of the membrane. Additionally, the increase in chemical shift from 185 ppm to 215 ppm upon incorporation of ^{15}N-[A380]hCB1 (T377-E416) into the longer-chain phospholipid bilayer indicates a substantial difference in orientation of the peptide between DMPC and POPC bilayers. The combined ^{15}N NMR and MD data support conclusion that the hCB1(T377-E416) peptide consists of two α-helical segments oriented nearly orthogonally to each other. These results are consistent with the high-resolution structure of the same peptide in DMPC bilayers with a peptide-to-lipid molar ratio of 1:50 (data not shown).

The helical tilt angle of hCB1(T377-E416) within the phospholipid bilayer environment was determined by using a total of six peptide samples, each with a single ^{15}N-labeled residue in the TM peptide segment. The labeled peptides were introduced into POPC and DMPC bilayers mechanically aligned between thin glass plates. Fig. 4 shows the orientation of all six (V378, A380, L388, V392, A398, L399) specific ^{15}N-labeled peptides within each membrane environment. The chemical shifts were extracted from the aligned spectra and recorded in Table 1 to aid calculation of the tilt angles. In POPC bilayers (Fig. 4A to F), the NMR spectra evidenced single line resonances with linewidths ranging from 6 to 20 ppm, suggesting a single conformation within the phospholipid bilayer. However, in DMPC bilayers, the resonance lines for the same sets of peptides are broad (Fig. 4G to L), suggesting conformational heterogeneity. This conformational distinction is supported by estimates made with the approach of Smith et al. [60] that the disorder in the alignment of the bilayers parallel to the glass plates (i.e., mosaic spread) is modest, ±0.3°. In both sets of spectra for DMPC and POPC bilayers, all selected residues exhibited ^{15}N peaks near the δ_{33} edge, indicating a TM hCB1(T377-E416) orientation. Increased tilt angles of peptides within membranes are often associated with decreased chemical shifts in aligned spectra [61]. In the current study, we indeed observed decreased chemical shifts in DMPC vs. POPC bilayers (Fig. 3).

The aligned ^{15}N chemical-shift measurements and the chemical-shift tensor elements from the unoriented DMPC and POPC spectra were used to determine precise protein helical tilt angles using established methods [62]. This determination was made with the assumption that hCB1(T377-E416) is a continuous α-helix within the membrane environment. As shown in the contour plots (Fig. 5), there is only one minimum identified to predict the orientation of hCB1(T377-E416) in DMPC and POPC bilayers. In Fig. 5A, the ^{15}N angle calculation shows a unique root-mean-square deviation (RMSD) minimum on the surface corresponding to $\tau = 26 \pm 2°$ and $\rho = -250°$ in DMPC and $\tau = 11 \pm 4°$ and $\rho = 50°$ in POPC. These values correspond to the most likely helical tilt orientations of hCB1(T377-E416) in DMPC and POPC bilayers.

Table 1
^{15}N chemical shift data [in ppm relative to $(^{15}NH_4)_2SO_4$ solution referenced to 27 ppm] from the single-site ^{15}N-labeled aligned samples of hCB1(T377-E416)

Membrane	Sites					
	V378	A380	L388	V392	A398	L399
DMPC	183	178	179	174	181	189
POPC	207	201	195	192	184	197

DMPC = mean values for triplicate scans for each residue ±3 ppm.
POPC = mean values for triplicate scans for each residue ±2 ppm.

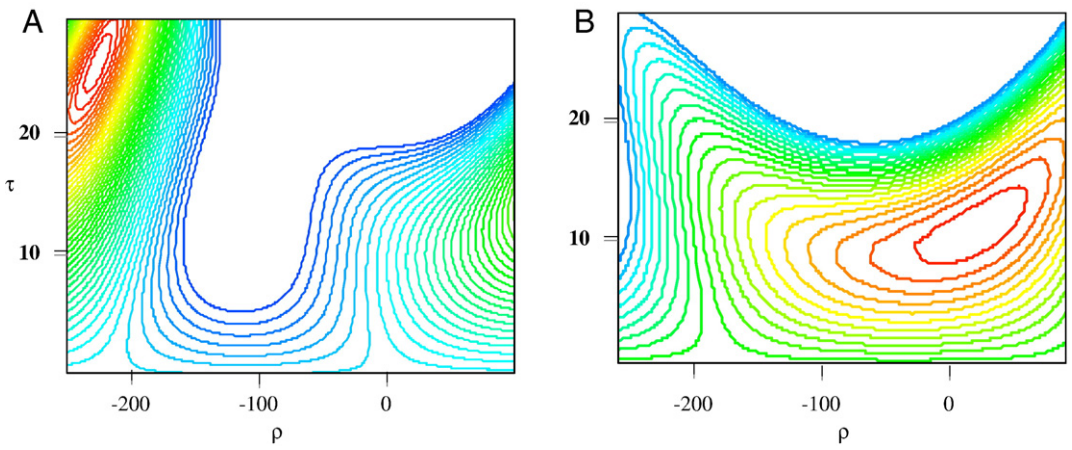

Fig. 5. Contour plots representing the ^{15}N chemical shifts calculated for the rotation, ρ from 0° to 360°, and for tilt angle, τ from 0° to 90°. The root-mean-square deviation (RMSD) between the experimental and calculated chemical shifts was calculated for each ρ and τ pair and plotted as τ (y-axis) versus ρ (x-axis). (A) The DMPC sample plot has a minimum at $\tau = 26°$ and $\rho = -250°$. (B) The POPC plot shows a minimum at $\tau = 11°$ and $\rho = 50°$.

3.3. MD simulations of hCB1(T377-E416) in DMPC and POPC

The difference in calculated tilt angles of hCB1(T377-E416) in DMPC vs. POPC bilayers may reflect the difference in phospholipid bilayer thickness. The DMPC bilayer carbonyl-to-carbonyl thickness is about 23 Å, whereas the POPC bilayer is 27 Å thick [63]. Thus, the transmembrane region of hCB1(T377-E416) might display greater tilt in the DMPC membrane than in the POPC membrane mimetic as a means to avoid hydrophobic mismatch between the shorter-chain DMPC lipid and the hydrophobic TM hCB1(T377-E416) region. In both MD simulations, helix 8 (D403-F412) is oriented parallel to the plane of the phospholipid membrane surface. The side-chains of the polar residues of the juxtamembrane segment (K402, H406, R409) are positioned among the head group region of the bilayer, whereas

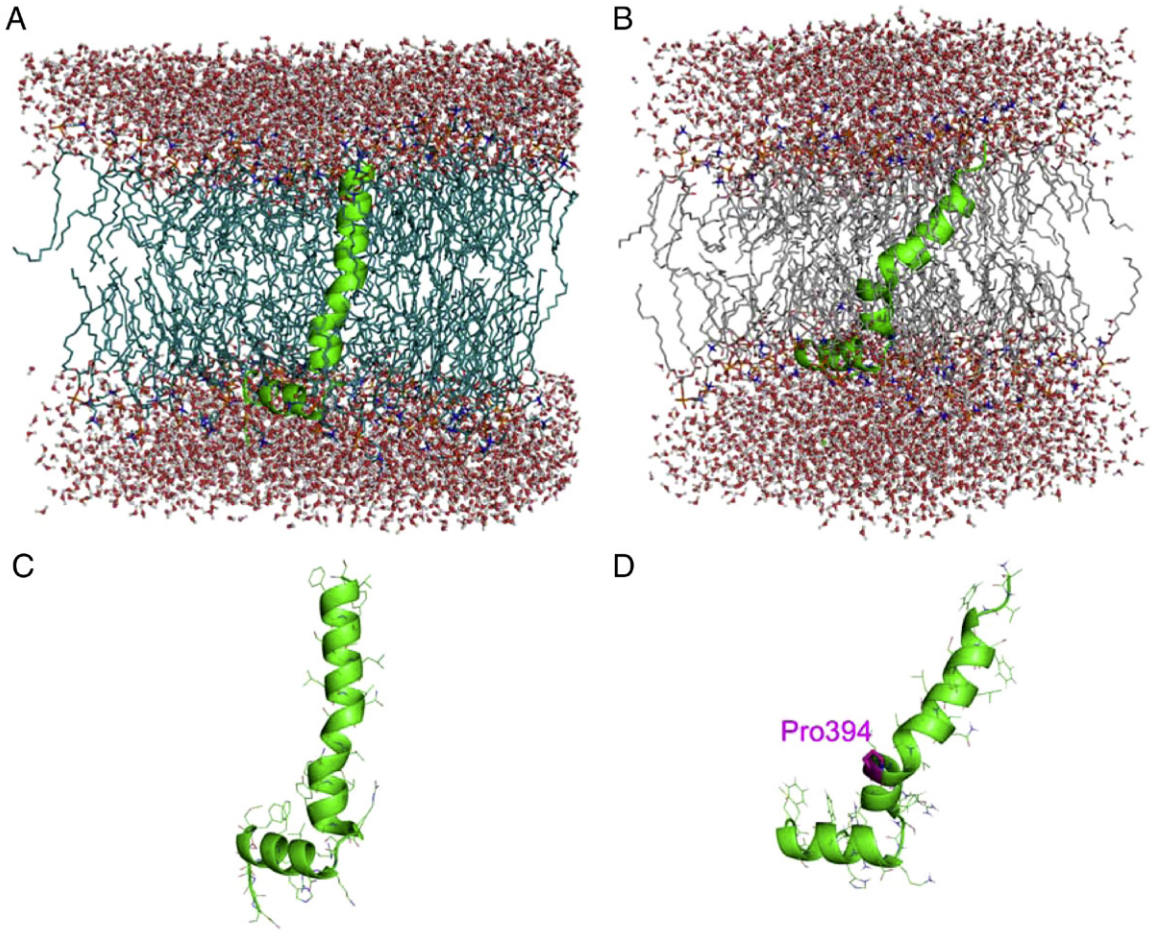

Fig. 6. Snapshots taken after 10-ns MD production of hCB1(T377-E416) in (A) POPC or (B) DMPC. The carbon atoms of POPC are shown in teal, whereas the carbon atoms of DMPC are shown in gray. hCB1(T377-E416) is shown in green. The shorter hydrophobic thickness of DMPC causes a kink in hCB1 (T377-E416) helix 7 at P394, as depicted in panels (C) vs. (D) without the membrane matrix.

the non-polar side-chains (L404, F408, M411) are in the lipophilic tail region of the bilayer. These peptide–lipid interactions appear to orient helix 8 in the bilayer. The side chain of R400 at the terminus of helix 7 forms a salt bridge to the phospholipid phosphate moiety, an interaction that may help tether the helix in the bilayer. The span of the POPC bilayer was sufficient to accommodate an extended TM helix 7 (T377-L399) within the membrane bilayer (Fig. 6A and C). In the thinner, DMPC bilayer (Fig. 6B), the TM region of hCB1(T377-E416) is kinked at P394 (Fig. 6D). From analysis of the MD trajectories, the tilt angle of helix 7 was determined to be $13 \pm 3°$ in the POPC bilayer and $28 \pm 5°$ in the DMPC bilayer. In the POPC bilayer, the angle between helices 7 and 8 was $89 \pm 5°$. In the DMPC bilayer, if the entirety of helix 7 is taken into account, the inter-helix angle was $119 \pm 7°$ because of the kink and helical tilt of the TM helix 7. However, the angle between helix 8 and the region of helix 7 proximal to it and beyond the kink was $89 \pm 4°$, similar to that found in the POPC bilayer.

3.4. Influence of membrane hydrophobic thickness on hCB1(T377-E416) backbone flexibility

The ^{15}N lineshapes in all ^{15}N-labeled sites for hCB1(T377-E416) in the DMPC environment were slightly broader than those obtained for the peptide in the POPC bilayer. This linewidth broadening may reflect factors such as increased mosaic spread and imperfection of the peptide's α-helical structure, which may result in conformational heterogeneity associated with differential protein–lipid interactions. Nonetheless, the aligned spectra clearly demonstrate that there are two hCB1(T377-E416) α-helices in two distinct environments. The semi-quantitative orientation of the helices with respect to each other is $91 \pm 6°$ in the POPC bilayer and $120 \pm 5°$ in the DMPC bilayer. These results compare favorably with the MD simulation data (above) and indicate that the two helices are roughly orthogonal to each other in their membrane environment. Nonetheless, caution should be exercised in comparing the MD and NMR data, for differences in the extent of hydration under the two experimental conditions may have influenced peptide insertion/conformation.

The orientation of hCB1 TM helix 7 within the membrane bilayer and relative to other hCB1 helices would likely influence ligand recognition by this GPCR. Indeed, a bend in TM helix 7 has been suggested to be critical for selective, high-affinity binding of CB1-receptor agonists [32]. We have defined in this study an energy-minimized interaction of hCB1(T377-E416) with DMPC and POPC bilayers. A key feature of the hCB1(T377-E416) peptide uncovered is its ability to orient TM helix 7 conformation cooperatively with its phospholipid bilayer environment to avoid hydrophobic mismatch. The transmembrane regions of most GPCRs contain conserved NP(X)nY motifs, and proline residues are α-helical destabilizers in globular proteins [10,11]. The TM NP(X)nY motif in hCB1 helix 7 could be important to the conformational changes we have observed in hCB1(T377-E416) between phospholipid membrane systems: it may allow a kink in a TM helix if helix tilting alone is not enough to relieve hydrophobic mismatch, especially in the case of a lengthy TM domain. Thus, multiple mechanisms could play a role in helix conformational changes to ensure hydrophobic matching by changing overall polypeptide span (Fig. 6). It is not surprising, therefore, that there are conserved proline residues in most GPCRs that might serve this purpose [10,11,64]. We postulate that the kink at P394 is crucial for conformational modulation of hCB1, which may occur in concert with additional structural rearrangements in other hCB1 helices. Since the present studies were performed in model membranes, however, the general relevance of these results to more complex and variable biological membrane environments will require future experimental confirmation.

4. Conclusion

Our solid-state NMR and computational data on the orientation of the 40-mer peptide hCB1(T377-E416) in a model membrane POPC bilayer clearly indicate that the first 23 amino acid residues, a segment of TM helix 7, form an α-helical structure embedded within the bilayer and oriented with a tilt angle of approximately 11° with respect to the normal membrane axis. The remaining amino acids constituting helix 8 are outside the hydrophobic core, approximately orthogonal to helix 7 and oriented parallel to the membrane surface. When hCB1(T377-E416) is introduced into a narrower (DMPC) bilayer membrane mimetic, a distinct change in the orientation of the peptide's TM segment was observed, with a greater tilt angle of 26°. The increased tilt reflected a response to avoid hydrophobic mismatch and was likely affected by a kink at P394. Our results thus constitute initial demonstration that the membrane bilayer plays a role in modulating the conformation and orientation of a CB-receptor TM helix. Given the importance of TM helix 7 to hCB1 ligand recognition [32], cooperative changes in the orientation of GPCR helices based on membrane thickness likely influence hCB1 function.

Acknowledgements

This work was supported by National Research Service Award Training Grant HL07917-06 from the National Institutes of Health (EKT) and grant DA3801 from the National Institute on Drug Abuse (AM). We thank William Beavers (Molecular Biology Core Facility, Dana-Farber Cancer Institute) for the peptide synthesis and purification, Drs. Alan Rigby and Amy Usheva for their valuable manuscript suggestions, and Drs. Sergiy Tyukhtenko, John Ladias, and Jerome Groopman for project support.

References

[1] S. Morein, E. Strandberg, J.A. Killian, S. Persson, G. Arvidson, R.E. Koeppe 2nd, G. Lindblom, Influence of membrane-spanning alpha-helical peptides on the phase behavior of the dioleoylphosphatidylcholine/water system, Biophys. J. 73 (1997) 3078–3088.
[2] O.G. Mouritsen, M. Bloom, Mattress model of lipid–protein interactions in membranes, Biophys. J. 46 (1984) 141–153.
[3] P.W. Hildebrand, R. Preissner, C. Frommel, Structural features of transmembrane helices, FEBS Lett. 559 (2004) 145–151.
[4] H.R. Pelham, S. Munro, Sorting of membrane proteins in the secretory pathway, Cell 75 (1993) 603–605.
[5] M.R.R. de Planque, D.V. Greathouse, R.E. Koeppe II, H. Schaffer, D. Marsh, J.A. Killian, Influence of lipid/peptide hydrophobic mismatch on the thickness of diacylphosphatidylcholine bilayers. A H-2 NMR and ESR study using designed transmembrane alpha-helical peptides and gramicidin A, Biochemistry 37 (1998) 9333–9345.
[6] A.G. Lee, Lipid–protein interactions in biological membranes: a structural perspective, Biochim. Biophys. Acta 1612 (2003) 1–40.
[7] Y.P. Zhang, R.N. Lewis, R.S. Hodges, R.N. McElhaney, Peptide models of helical hydrophobic transmembrane segments of membrane proteins. 2. Differential scanning calorimetric and FTIR spectroscopic studies of the interaction of Ac-K2-(LA)12-K2-amide with phosphatidylcholine bilayers, Biochemistry 34 (1995) 2362–2371.
[8] M. Venturoli, B. Smit, M.M. Sperotto, Simulation studies of protein-induced bilayer deformations, and lipid-induced protein tilting, on a mesoscopic model for lipid bilayers with embedded proteins, Biophys. J. 88 (2005) 1778–1798.
[9] D. Marsh, Protein modulation of lipids, and vice versa, in membranes, Biochim. Biophys. Acta 1778 (2008) 1545–1575.
[10] G. Vanhoof, F. Goossens, I. de Meester, D. Hendriks, S. Scharpé, Proline motifs in peptides and their biological processing, FASEB J. 9 (1995) 736–744.
[11] K. Konvicka, F. Guarnieri, J.A. Ballesteros, H. Weinstein, A proposed structure for transmembrane segment 7 of G protein-coupled receptors incorporating an Asn-Pro/Asp-Pro motif, Biophys. J. 75 (1998) 610–611.
[12] T. Bisogno, Endogenous cannabinoids: structure and metabolism, J. Neuroendocrinol. 20 (2008) 1–9.
[13] K. Mackie, Cannabinoid receptors: where they are and what they do, J. Neuroendocrinol. 20 (Suppl. 1) (2008) 10–14.
[14] R.G. Pertwee, The pharmacology of cannabinoid receptors and their ligands: an overview, Int. J. Obes. 30 (2006) S13–S18.
[15] V.K. Vemuri, D.R. Janero, A. Makryannis, Pharmacotherapeutic targeting of the endocannabinoid signaling system: drugs for obesity and the metabolic syndrome, Physiol. Behav. 93 (2008) 671–686.

[16] S.M. Wright, C. Dikkers, L.J. Aronne, Rimonabant: new data and emerging experience, Curr. Atheroscler. Rep. 10 (2008) 71–78.
[17] A. Kapur, P. Samaniego, G.A. Thakur, A. Makriyannis, M.E. Abood, Mapping the structural requirements in the CB1 cannabinoid receptor transmembrane helix II for signal transduction, J. Pharmacol. Exp. Ther. 325 (2008) 341–348.
[18] R.A. Ross, Tuning the endocannabinoid system: allosteric modulators of the CB1 receptor, Br. J. Pharmacol. 152 (2007) 565–566.
[19] X.Q. Xie, J.Z. Chen, E.M. Billings, 3D structural model of the G-protein-coupled cannabinoid CB2 receptor, Proteins 53 (2003) 307–319.
[20] K. Wakamatsu, D. Kohda, H. Hatanaka, J.M. Lancelin, Y. Ishida, M. Oya, H. Nakamura, F. Inagaki, K. Sato, (1992) Structure–activity relationships of muconotoxin GIIIA: structure determination of active and inactive sodium channel blocker peptides by NMR and simulated annealing calculations, Biochemistry 31 (1992) 12577–12584.
[21] J. Klein-Seetharaman, N.V.K. Yanamala, F. Javeed, P.J. Reeves, E.V. Getmanova, M.C. Loewen, H. Schwalbe, H.G. Khorana, Differential dynamics in the G protein-coupled receptor rhodopsin revealed by solution NMR, Proc. Natl. Acad. Sci. U. S. A. 101 (2004) 3409–3413.
[22] K. Palczewski, T. Kumasaka, T. Hori, C.K. Behnke, H. Motoshima, B.A. Fox, I. Le Trong, D.C. Teller, T. Okada, R.E. Stenkamp, M. Yamamoto, M. Miyano, Crystal structure of rhodopsin: a G protein-coupled receptor, Science 289 (2000) 739–745.
[23] V. Cherezov, D.M. Rosenbaum, M.A. Hanson, S.G. Rasmussen, F.S. Thian, T.S. Kobilka, H.J. Choi, P. Kuhn, W.I. Weis, B.K. Kobilka, R.C. Stevens, High-resolution crystal structure of an engineered human β2-adrenergic G protein-coupled receptor, Science 318 (2007) 1258–1265.
[24] J.H. Park, P. Scheerer, K.P. Hofmann, H.-W. Choe, O.P. Ernst, Crystal structure of the ligand-free G-protein-coupled receptor opsin, Nature 455 (2008) 497–502.
[25] T. Warne, M.J. Serrano-Vega, J.G. Baker, R. Moukhametzianov, P.C. Edwards, R. Handerson, A.G.W. Leslie, C.G. Tate, G.F.X. Schertler, Structure of a β_1-adrenergic G-protein-coupled receptor, Nature 454 (2008) 486–491.
[26] A. Poso, J.W. Huffman, Targeting the cannabinoid CB2 receptor: modeling and structural determinants of CB2 selective ligands, Br. J. Pharmacol. 153 (2008) 335–346.
[27] P.H. Reggio, Computational methods in drug design: modeling G protein-coupled receptor monomers, dimers, and oligomers, AAPS J. 8 (2006) E322–E336.
[28] R.D. Bramblett, A.M. Panu, J.A. Ballesteros, P.H. Reggio, Construction of a 3D model of the cannabinoid CB1 receptor: determination of helix ends and helix orientation, Life Sci. 56 (1995) 1971–1982.
[29] G. Choi, J. Guo, A. Makriyannis, The conformation of the cytoplasmic helix 8 of the CB1 cannabinoid receptor using NMR and circular dichroism, Biochim. Biophys. Acta 1668 (2005) 1–9.
[30] R.P. Picone, A.D. Khandolar, W. Xu, L.A. Ayotte, G.A. Thakur, D.P. Hurst, M.E. Abood, P.H. Reggio, D.J. Fournier, A. Makriyannis, (−)-7′-Isothiocyanato-11-hydroxy-1′,1′-dimethylheptylhexahydrocannabinol (AM841), a high-affinity electrophilic ligand, interacts covalently with a cysteine in helix six and activates the CB1 cannabinoid receptor, Mol. Pharmacol. 68 (2005) 1623–1635.
[31] S.D. McAllister, G. Rizvi, S. Anavi-Goffer, D.P. Hurst, J. Barnett-Norris, D.L. Lynch, P.H. Reggio, M.E. Abood, An aromatic microdomain at the cannabinoid CB(1) receptor constitutes an agonist/inverse agonist binding region, J. Med. Chem. 46 (2003) 5139–5152.
[32] A. Kapur, D.P. Hurst, D. Fleischer, R. Whitnell, G.A. Thakur, A. Makriyannis, P.H. Reggio, M.E. Abood, Mutation studies of Ser7.39 and Ser2.60 in the human CB1 cannabinoid receptor: evidence for a serine-induced bend in CB1 transmembrane helix 7, Mol. Pharmacol. 71 (2007) 1512–1524.
[33] A. Gonzalez, L.S. Duran, R. Araya-Secchi, J.A. Garate, C.D. Pessoa-Mahana, C.F. Lagos, T. Perez-Acle, Computational modeling study of functional microdomains in cannabinoid receptor type 1, Bioorg. Med. Chem. 16 (2008) 4378–4389.
[34] B.A. Cornell, F. Separovic, A.J. Baldassi, R. Smith, Conformation and orientation of gramicidin A in oriented phospholipid bilayers measured by solid state carbon-13 NMR, Biophys. J. 53 (1988) 67–76.
[35] R. Smith, F. Separovic, T.J. Milne, A. Whittaker, F.M. Bennett, B.A. Cornell, A. Makriyannis, Structure and orientation of the pore-forming peptide, melittin, in lipid bilayers, J. Mol. Biol. 241 (1994) 456–466.
[36] C.T. Chang, C.-S. Wu, J.T. Yang, Circular dichroism analysis of protein conformation inclusion of the beta-turns, Anal. Biochem. 91 (1978) 13–31.
[37] S.R. Martin, M.J. Schilstra, Circular dichroism and its application to the study of biomolecules, Methods Cell Biol. 84 (2008) 263–293.
[38] Y.H. Chen, J.T. Yang, K.H. Chau, Determination of the helix and beta form of proteins in aqueous solution by circular dichroism, Biochemistry 13 (1974) 3350–3359.
[39] S.J. Opella, P.L. Stewart, Solid-state nuclear magnetic resonance structural studies of proteins, Methods Enzymol. 179 (1989) 242–275.
[40] A. Makriyannis, A. Banijamali, C. Van der Schyf, H. Jarrell, Interactions of cannabinoids with membranes. The role of cannabinoid stereochemistry and absolute configuration and the orientation of delta-9-THC in the membrane bilayer, NIDA Res. Monogr. 79 (1987) 123–133.
[41] E.K. Tiburu, E.S. Karp, G. Birrane, J.O. Struppe, S. Chu, G.A. Lorigan, S. Avraham, H.K. Avraham, ^{31}P and ^{2}H relaxation studies of helix VII and the cytoplasmic helix of the human cannabinoid receptors utilizing solid-state NMR techniques, Biochemistry 45 (2006) 7356–7365.
[42] E.K. Tiburu, E.S. Karp, P.C. Dave, K. Damodaran, G.A. Lorigan, Investigating the dynamic properties of the transmembrane segment of phospholamban incorporated into phospholipid bilayers utilizing ^{2}H and ^{15}N solid-state NMR spectroscopy, Biochemistry 43 (2004) 13899–13909.
[43] A. Mascioni, C. Karim, G. Barany, D.D. Thomas, G. Veglia, Structure and orientation of sarcolipin in lipid environments, Biochemistry 41 (2002) 475–482.
[44] E. Strandberg, S. Ozdirekcan, D.T.S. Rijkers, P.C.A. van der Wel, R.E. Koeppe II, R.M.J. Liskamp, J.A. Killian, Tilt angles of transmembrane model peptides in oriented and non-oriented lipid bilayers as determined by 2H solid-state NMR, Biophys. J. 86 (2004) 3709–3721.
[45] J.A. Whiles, K.J. Glover, R.R. Vold, E.A. Komives, Methods for studying transmembrane peptides in bicelles: consequences of hydrophobic mismatch and peptide sequence, J. Magn. Reson. 158 (2002) 149–156.
[46] J.A. Whiles, R. Brasseur, K.J. Glover, G. Melacini, E.A. Komives, R.R. Vold, Orientation and effects of mastoparan X on phospholipid bicelles, Biophys. J. 80 (2001) 280–293.
[47] D.H. Jones, K.R. Barber, E.W. VanDerLoo, W.M. Grant, Epidermal growth factor receptor transmembrane domain: 2H NMR implications for orientation and motion in a bilayer environment, Biochemistry 37 (1998) 16780–16787.
[48] D.P. Tieleman, M.S.P. Sansom, H.J.C. Berendsen, Alamethicin helices in a bilayer and in solution: molecular dynamics simulations, Biophys. J. 76 (1999) 40–49.
[49] J.M. Smaby, M.M. Momsen, H.L. Brockman, R.E. Brown, Phosphatidylcholine acyl unsaturation modulates the decrease in interfacial elasticity induced by cholesterol, Biophys. J. 73 (1997) 1492–1505.
[50] H.J.C. Berendsen, J.P.M. Postma, W.F. Vangunsteren, A. Dinola, J.R. Haak, Molecular-dynamics with coupling to an external bath, J. Chem. Phys. 81 (1984) 3684–3690.
[51] T. Darden, D. York, L. Pedersen, Particle Mesh Ewald — an *N*.Log(*N*) method for Ewald sums in large systems, J. Chem. Phys. 98 (1993) 10089–10092.
[52] U. Essmann, L. Perera, M.L. Berkowitz, T. Darden, H. Lee, L.G. Pedersen, A smooth Particle Mesh Ewald method, J. Chem. Phys. 103 (1995) 8577–8593.
[53] B. Hess, H. Bekker, H.J.C. Berendsen, J. Fraaije, LINCS: a linear constraint solver for molecular simulations, J. Comput. Chem. 18 (1997) 1463–1472.
[54] H.J.C. Berendsen, J.P.M. Postma, W.F. van Gunsteren, J. Hermans, Interaction models for water in relation to protein hydration, in: B. Pullman (Ed.), Intermolecular Forces, Reidel, Dordrecht, 1981, pp. 331–342.
[55] O. Berger, O. Edholm, F. Jahnig, Molecular dynamics simulations of a fluid bilayer of dipalmitoylphosphatidylcholine at full hydration, constant pressure, and constant temperature, Biophys. J. 72 (1997) 2002–2013.
[56] S.W. Chiu, M. Clark, V. Balaji, S. Subramaniam, H.L. Scott, E. Jakobsson, Incorporation of surface tension into molecular dynamics simulation of an interface — a fluid-phase lipid bilayer membrane, Biophys. J. 69 (1995) 1230–1245.
[57] W.F. van Gunsteren, S.R. Billeter, A.A. Eising, P.H. Hünenberger, P. Krüger, A.E. Mark, W.R.P. Scott, I.G. Tironi, Biomolecular Simulation: the GROMOS96 Manual and User Guide, vdf Hochschulverlag AG, Zürich, 1996.
[58] H.J.C. Berendsen, D. Vanderspoel, R. Vandrunen, Gromacs — a message-passing parallel molecular-dynamics implementation, Comput. Phys. Commun. 91 (1995) 43–56.
[59] E. Lindahl, B. Hess, D. van der Spoel, GROMACS 3.0: a package for molecular simulation and trajectory analysis, J. Mol. Model. 7 (2001) 306–317.
[60] R. Smith, F. Separovic, F.C. Bennett, B.A. Cornell, Melittin-induced changes in lipid multilayers. A solid-state NMR study, Biophys. J. 63 (1992) 469–474.
[61] S. Morein, I.R. Koeppe, G. Lindblom, B. de Kruijff, J.A. Killian, The effect of peptide/lipid hydrophobic mismatch on the phase behavior of model membranes mimicking the lipid composition in *Escherichia coli* membranes, Biophys. J. 78 (2000) 2475–2485.
[62] F.A. Kovacs, J.K. Denny, Z. Song, J.R. Quine, T.A. Cross, Helix tilt of the M2 transmembrane peptide from influenza A virus: an intrinsic property, J. Mol. Biol. 295 (2000) 117–125.
[63] B.A. Cornell, F. Separovic, Membrane thickness and acyl chain length, Biochim. Biophys. Acta 733 (1983) 189–193.
[64] M.R.R. de Planque, D.T.S. Rijkers, J.I. Fletcher, R.M.J. Liskamp, F. Separovic, The αM1 segment of the nicotinic acetylcholine receptor exhibits conformational flexibility in a membrane environment, Biochim. Biophys. Acta 1665 (2004) 40–47.